Title

Evaluating the effect of pulse energy on femtosecond laser trabeculotomy (FLT) outflow channels for glaucoma treatment in human cadaver eyes.

Journal

Lasers in Surgery and Medicine, 56(4)

Authors

Luo, Shangbang
Mikula, Eric
Khazaeinezhad, Reza
et al.

Publication Date

2024-04-01

DOI

10.1002/lsm.23783

Peer reviewed

HHS Public Access

Author manuscript

Lasers Surg Med. Author manuscript; available in PMC 2025 April 03.

Published in final edited form as:

Lasers Surg Med. 2024 April ; 56(4): 382–391. doi:10.1002/lsm.23783.

Evaluating the Effect of Pulse Energy on Femtosecond Laser Trabeculotomy (FLT) Outflow Channels for Glaucoma Treatment in Human Cadaver Eyes

Shangbang Luo[1,2], **Eric R. Mikula**[2,3], **Reza Khazaeinezhad**[3], **Samantha M. Bradford**[2], **Fengyi Zhang**[1,4], **James V. Jester**[1,2], **Tibor Juhasz**[1,2,3,*]

[1]Department of Biomedical Engineering, University of California, Irvine, Irvine, CA 92697, USA

[2]Department of Ophthalmology, University of California, Irvine, Irvine, CA 92697, USA

[3]ViaLase Inc., Aliso Viejo, CA 92656, USA

[4]Beckman Laser Institute, University of California, Irvine, Irvine, CA 92697, USA

Abstract

Background and Objectives: Femtosecond laser trabeculotomy (FLT) creates aqueous humor outflow channels through the trabecular meshwork (TM) and is an emerging non-invasive treatment for open-angle glaucoma. The purpose of this study is to investigate the effect of pulse energy on outflow channel creation during FLT.

Materials and Methods: An FLT laser (ViaLase Inc., Aliso Viejo, CA) was used to create outflow channels through the TM (500 μm wide by 200 μm high) in human cadaver eyes using pulse energies of 10, 15, and 20 μJ. Following treatment, tissues were fixed in 4% paraformaldehyde (PFA). The channels were imaged using optical coherence tomography (OCT) and assessed as full thickness, partial thickness, or not observable.

Results: Pulse energies of 15 μJ and 20 μJ had a 100% success rate in creating full-thickness FLT channels as imaged by OCT. A pulse energy of 10 μJ resulted in no channels (n=6), a partial-thickness channel (n=2), and a full-thickness FLT channel (n=2). There was a statistically significant difference in cutting widths between the 10 μJ and 15 μJ groups ($P < 0.0001$), as well as between the 10 μJ and 20 μJ groups ($P < 0.0001$). However, there was no statistically significant difference between the 15 μJ and 20 μJ groups ($P = 0.416$).

Conclusions: 15 μJ is an adequate pulse energy to reliably create aqueous humor outflow channels during FLT in human cadaver eyes. OCT is a valuable tool when evaluating FLT.

Keywords

Femtosecond laser trabeculotomy (FLT); energy optimization; trabecular meshwork; outflow channel; OCT; glaucoma; human cadaver eyes

*Corresponding author: tjuhasz@hs.uci.edu, 843 Health Sciences Road, University of California, Irvine, CA, USA.

1. INTRODUCTION

Glaucoma is a disease characterized by the death of retinal ganglion cells, optic nerve head cupping, and is often associated with elevated intraocular pressure (IOP)[1]. The only proven treatment for glaucoma is the reduction of IOP[2]. IOP is the result of a balance between aqueous humor secretion by the ciliary processes and the outflow of aqueous humor through the trabecular meshwork (TM) and Schlemm's canal (SC), and to a lesser degree, the uveoscleral pathway. It is thought that most of the resistance to aqueous humor outflow is found in the juxtacanalicular region of the TM and inner wall of SC[3–6]. As such, numerous devices and procedures aim to bypass the resistance found in these tissues with the goal of lowering IOP[7–11]. Though these methods achieve an IOP reduction, they are all, except selective laser trabeculoplasty, invasive to a degree because they require opening the eye to either insert surgical instrumentation or an implant. Recently, femtosecond laser trabeculotomy (FLT) has emerged as a non-invasive, non-incisional method to bypass aqueous humor outflow resistance[12–14].

The use of a femtosecond laser for glaucoma treatment has several advantages. Firstly, a tightly focused femtosecond laser beam enables photodisruption or laser-induced optical breakdown to occur only at a well-defined focal spot, resulting in localized and confined tissue removal[15]. Secondly, the pulse duration and plasma expansion time associated with femtosecond lasers are shorter than the local thermal diffusion time, leading to limited thermal damage[16]. Lastly, experimental studies on human ocular tissues have demonstrated that femtosecond lasers produce reduced shock wave and cavitation bubble effects compared to lasers with longer pulse durations, resulting in minimal localized tissue damage[15]. These favorable properties, coupled with the ability to non-invasively deliver the laser pulse and the precise scanning and delivery control enabled by modern computer systems, make femtosecond lasers an ideal technique for trabecular bypass surgery. Furthermore, the safety and efficacy of femtosecond laser have been demonstrated over the last twenty years for various procedures, including flap creation in corneal refractive surgery, capsulotomy, lens fragmentation, and corneal incisions during cataract surgery[17–20].

The use of femtosecond lasers to perform trabeculotomy enables dynamic delivery of tightly focused laser pulses through the cornea, across the anterior chamber, and to SC[12,13,21,22]. This innovative approach non-invasively establishes a conduit between the anterior chamber and SC, thus providing an unobstructed aqueous humor outflow channel. Though initial studies in cadaver eye perfusion models have shown promising IOP reductions, the optimal pulse energy required for successful FLT surgery needs to be investigated. In this study, we use OCT to investigate the influence of pulse energy on the creation of outflow channels within the TM during FLT surgery in human cadaver eyes.

2. MATERIALS AND METHODS

2.1 FLT Delivery System

The FLT system consists of several components, including a femtosecond laser, a gonioscopic camera, a low power HeNe aiming laser, and a series of optics, as depicted in Fig.1. For our experiments, we utilized a commercial amplified diode-pumped Ytterbium-

based femtosecond laser (Origami-10XP Femtosecond Laser, NKT Photonics, Denmark). This laser emits pulses with a duration of 400 fs, a wavelength of 1.03 μm, and a pulse repetition frequency of 10 kHz.

The laser light passes through a beam expander (a|BeamExpander, Asphericon, Germany) to dilate the beam radius and fill the aperture of the objective. The beam scanning in the TM area is controlled by a pair of galvo-scanners, which determine the horizontal (X-axis) and vertical (Y-axis) directions. An objective lens focuses the laser beam through a custom gonioscopic lens into iridocorneal angle (spot size < 10μm). Additionally, a video camera is integrated into the system to facilitate real-time guidance by providing direct visualization of the iridocorneal angle structures. The femtosecond surgical beam is guided by a coaxial 5 mW, 632.8 nm HeNe dual aiming laser (Thorlabs, Inc., Newton, NJ, USA). The convergence of the dual beams onto the TM serves as an indication of the focal plane of the femtosecond laser.

Figure 2 provides a schematic diagram illustrating the creation of the femtosecond channel and its dimensional relationship to the structures in the iridocorneal angle. Photodisruption occurs within a confined region corresponding to the beam focus size. This process is repeated as the femtosecond laser focus is scanned in a continuous rectangular volume through the TM tissues, resulting in the creation of a patent femtosecond channel connecting the anterior chamber (AC) to SC. The dimensions of the channel are determined by the channel width (W) in the horizontal direction (X-axis), and the channel height (H) in the vertical direction (Y-axis).

2.2 Human Cadaver Eye Samples Preparation

Six human cadaver eyes, which were not suitable for transplant, were obtained from the San Diego Eye Bank within 24 hours postmortem. Careful dissection was performed to preserve the TM while removing other ocular components, including the posterior segment, vitreous, lens, iris, ciliary body, choroid, and uveal tissues (Fig. 3A). Note that the TM is anchored posteriorly into the relatively stiff scleral spur, which provides a mechanical and physical boundary between the TM and ciliary body/iris. Thus in the ex-vivo case, the removal of these tissues should not have an appreciable effect on the mechanics of the TM or the photodisruptive ability of the femtosecond laser. Subsequently, the prepared eyes were stored in Optisol GS corneal transplant medium (Chiron Intraoptics, Irvine, CA) and refrigerated at 4°C (Fig. 3B). The experimental procedures adhered to the principles outlined in the Declaration of Helsinki.

To assess morphology and viability, the cadaver eyes were examined under an optical microscope before being mounted on a custom sample holder. The eyes were then perfused with Dulbecco's modified Eagle's medium (DMEM) containing 5 μg/mL amphotericin B and 100 μg/mL streptomycin (MilliporeSigma, MO) in a sterile tissue culture incubator (Sheldon Manufacturing, Inc., Cornelius, OR) at 37°C, 5% CO_2, and 95% humidity for 30 minutes (Fig. 3C). The corneal epithelium was removed due to irregularities in the surface quality. It should be noted that the perfusion system was strictly monitored to ensure the absence of bubbles or leakage, as these could impede the subsequent surgical procedure.

2.3 Femtosecond Laser Channel Creations in Human Cadaver Eyes

The eye was subsequently placed on a movable mechanical stage/sample holder equipped with five degrees of freedom, including x, y, z translations, rotation, and tilting, within the FLT laser surgery system (Fig. 3D). To optimize optical performance and provide a protective barrier, a custom-built patient interface was used between the laser system and the human cadaver eye, minimizing aberrations and reflective losses. Additionally, a drop of index-matching gel (GenTeal Gel, Novartis, Basel, Switzerland) was applied between the patient interface and the gonioscopic lens to reduce optical reflections at the interfaces. To ensure clear visualization of the TM and surrounding tissues at the iridocorneal angle, a drop of 20% dextran was directly applied to the eye to mitigate corneal edema.

Before commencing the surgical procedure, meticulous adjustments of the gonioscopic camera and sample holder were made to visualize the TM at the iridocorneal angle. Once the TM was visible, the dual aiming beams were aligned to overlap onto the TM surface, targeting the treatment laser. In this study, pulse energies of 10, 15, and 20 μJ were used, and channels with dimensions of W×H=500×200 μm^2 were created. When the laser shutter was opened, the femtosecond laser beam initiated photodisruption through the TM, starting from inside SC and moving out towards the anterior chamber (AC), following a preprogrammed raster pattern controlled by the computer. The formation of an outflow channel took several seconds, depending on the laser scanning parameters and drainage geometry. Each eye received 5 channels at a particular energy.

After completing the surgical procedure, the surgical position was marked to facilitate subsequent OCT imaging. Following the treatments, the eyes were fixed in 4% PFA (Mallinckrodit Baker, Inc., Phillipsburg, NJ) in phosphate-buffered saline (PBS) and dissected for post-surgery OCT imaging experiments.

2.4 OCT Imaging

In this study, we used a spectral domain OCT to evaluate the created channels. The imaging system operates at an A-line rate of 50 kHz and has a central wavelength of 890 nm, offering a theoretical axial resolution of 2.4 μm[23]. The tissue sample was immersed in the PBS solution and carefully adjusted so that the OCT beam was scanned approximately perpendicular to the width of the surgical site.

2.5 Quantifying and Visualizing the Created Channels by OCT

To assess the efficacy and precision of channel creation using the femtosecond beam, we conducted an evaluation of the OCT image stacks corresponding to the FLT channel (Fig. 4D). The evaluation was performed by analyzing the B-scan image slices individually (Fig. 4). We defined a continuous cutting width (W_c) of at least 200 μm within the desired 500 μm channel width as a complete drainage channel connecting to the SC, indicating a full-thickness cut. Any width below this threshold indicated either partial thickness cuts or the absence of observable outflow channels (refer to Fig. 5).

Furthermore, the acquired image stacks were cropped to a volume size of V_{xyz} =1×1×1 mm^3, with the FLT outflow channel positioned at the center of the selected volumetric

image. In the context of OCT imaging, z represents the depth direction, x corresponds to the fast scan direction, and y indicates the slow scan direction between B-scans. Subsequently, the image stacks were imported into FluoRender 2.25.2 software (Scientific Computing and Imaging Institute, Salt Lake City, UT, USA) for 3-D rendering. To enhance the visual representation, the 'Hot Effect' was applied along the depth in the software settings, facilitating the three-dimensional visualization.

2.6 Statistics

Unpaired *t*-tests using GraphPad Prism 10 (GraphPad Software, Boston, MA, USA) were conducted to examine potential significant differences in the cutting widths associated with different FLT pulse energies (10 μJ vs. 15 μJ, 10 μJ vs. 20 μJ, and 15 μJ vs. 20 μJ).

3. RESULTS

3.1 Representative Outflow Channels Under a Light Microscope

Images of outflow channels taken through an operating microscope are shown in Fig. 6; channels are indicated by double arrows. These channels were created by irradiating the brownish TM with 15 μJ pulse energy using FLT surgery in a human donor eye. The corneoscleral shell was imaged at an angle, with the endothelium facing upward, allowing for the direct capture of the TM by the optical microscope. While these images nicely demonstrate the location of the outflow channels, a more detailed assessment is required to determine whether the channels were fully cut by the FLT surgery. This evaluation can be achieved through a closer and deeper examination using a 3D OCT imaging modality, as reported below.

3.2 OCT Evaluation of Femtosecond Laser Channel Creations at Varying Pulse Energies

Figure 7 shows sample OCT images of FLT outflow channels at different pulse energies. In this specific case, the representative FLT channel created at 10 μJ pulse energy was partially cut by the femtosecond laser, while the channels at 15 μJ and 20 μJ cut through the entire TM into SC.

The mean ± standard deviation cutting widths of the outflow channels through the TM were 74 ± 157, 403 ± 89, and 368 ± 99 μm for the 10 μJ, 15 μJ, and 20 μJ energy groups, respectively. These results are summarized in Fig. 8. Significantly different cutting widths were observed between the 10 μJ and 15 μJ groups ($P < 0.0001$), as well as between the 10 μJ and 20 μJ groups ($P < 0.0001$). However, there was no significant difference between the 15 μJ and 20 μJ groups ($P = 0.416$).

Comprehensive data regarding all FLT channel creations are presented in Table 1. The results indicate that pulse energies of 15 μJ and 20 μJ achieved a 100% success rate in creating full-thickness FLT channels with a continuous cutting width of at least 200 μm, as confirmed by OCT imaging. In contrast, the use of 10 μJ pulse energy resulted in the absence of channels in 6 cases, partial-thickness channels in 2 cases, and complete FLT channels in 2 cases.

3.3 Three-Dimensional OCT Representation of the Femtosecond Laser Outflow Channels and Iridocorneal Angle Structures

For a comprehensive understanding of the complete profile of the FLT channel at the iridocorneal angle, a three-dimensional visualization of a 1×1 mm^2 segment of the corneoscleral rim is provided in Fig. 9. In this representation, the SC appeared as a patent tube (Fig. 9A and B), accompanied by the overlaying TM tissue. Importantly, the OCT reconstruction clearly reveals a wedge-shaped channel created by the femtosecond laser. The TM is fully penetrated with sharp edges, resulting in direct exposure of SC to the aqueous humor in the anterior chamber (AC).

4. DISCUSSION

In this study, we employed OCT to assess the impact of pulse energy on the creation of outflow channels during FLT surgery in human cadaver eyes. Our aim was to determine the optimized energy level for the surgical procedure. Overall, the present study demonstrated that pulse energy significantly influenced the creation of outflow channels during FLT surgery in human cadaver eyes, resulting in variations such as full thickness, partial thickness, or absence of observable channels, as observed through spectral domain OCT imaging (see Table 1, Fig. 7). By evaluating the OCT images, we have determined that a pulse energy of 15 μJ reliably achieves the creation of outflow channels by photodisrupting the TM tissues in human cadaver eyes. Conversely, lower energy levels, such as 10 μJ, do not guarantee the attainment of full thickness cutting through the TM tissues. Typically, using the least amount of energy to accomplish a surgery is considered optimal. Any amount of energy over the minimum necessary, though it may not be damaging, is unneeded. These findings have potential implications for guiding the choice of pulse energy in the clinical setting.

Previous groups had explored using femtosecond laser to non-invasively bypass aqueous outflow resistance with limited success. Researchers have employed 800 nm femtosecond laser pulses focused directly through air onto the exposed TM within a 4-mm excised strip of the porcine corneoscleral rim[24]. Histological analysis revealed successful photodisruption of the TM, including the juxtacanalicular tissue, using moderate pulse energies of 7 to 14 μJ and short exposure times ranging from 0.5 to 2 seconds. While this study successfully removed TM with a femtosecond laser, it was not conducted in a clinically relevant manner through the intact cornea. The same group also investigated the feasibility of photodisrupting the TM using femtosecond laser pulses focused through a goniolens with significantly higher energies of 60–480 μJ[25]. However, histological results indicated that they were unable to reach the innermost layer of the TM known as the juxtacanalicular tissue and the inner wall of SC, which are believed to contribute to the greatest resistance to aqueous outflow[3,26]. This failure may be attributed to the lack of necessary optimization of the focal spot size of the femtosecond laser beam propagating through the gonioscopic contact lens, cornea, and anterior chamber, as well as the absence of proper visualization of the iridocorneal angle structures.

Researchers have used two-photon or histological imaging to evaluate the femtosecond laser created channels[24,25,27]. However, both imaging techniques necessitate tissue sectioning

and face challenges in determining the continuous and overall cutting profile of the entire FLT channel. OCT has demonstrated its capability for three-dimensional imaging of the entire femtosecond-created channels in human cadaver eye tissues[12]. Moreover, our previous experience utilizing a custom-built spectral domain OCT to provide detailed visualization of the iridocorneal angle structures[28,29], supports the suitability of OCT for this investigation. As discussed in this study, OCT has been employed as an effective tool to evaluate the impact of pulse energy on the generation of outflow channels during FLT surgery in human cadaver eyes. Furthermore, OCT has successfully aided in determining the optimal energy level for the FLT procedure. A three-dimensional OCT reconstruction clearly depicted the location of the outflow channel within the TM, thus establishing a direct connection between SC to aqueous fluid in the anterior chamber (see Fig. 9). This raises a possibility that OCT can be translated for evaluations of the clinical laser surgery for the treatment of glaucoma. Further investigation of OCT imaging follow-ups is needed to assess the long-term outcomes after surgery[14].

It is important to discuss the acceptance criteria defined in this study for a “full channel”, which was defined as a channel with a continuous cutting width of at least 200 μm fully penetrating the TM into SC. Since the channel width defined in the experiment is 500 μm, one would reasonably expect that the success criteria would be closer to 500 μm. The criteria of 200 μm or greater is borne from prior laboratory experience in passing femtosecond pulse obliquely through the cadaver cornea, across the anterior chamber, and to the TM[30,31]. Though we employed strict acceptance criteria and handling procedures regarding the donor cadaver tissue, there still exists uncontrollable variability in the quality of the corneas, specifically the viability of the endothelium and surface quality of the cornea. Endothelial function directly affects corneal clarity and edema. Additionally, cadaver corneoscleral rims are subject to wrinkling on the posterior corneal surface. The consequence of these defects is variability in the quality of the trabeculotomy in the tissue. Taking into consideration the variability of these tissues, one would not expect full-width cuts all the time, as shown by the data in Table 1. For example, in living tissue, the corneas could be expected to be clearer than cadaver corneas and therefore may achieve more complete cuts in lower energies.

5. CONCLUSIONS

In conclusion, this study successfully demonstrated the capability of our FLT system, utilizing a pulse energy of 15 μJ, to effectively photodisrupt the TM tissues. This resulted in the creation of a full-thickness outflow channel, establishing a vital connection between the anterior chamber and SC. Confirmation of this outcome was achieved through a comprehensive analysis of high-resolution OCT images. These findings underscore the effectiveness of utilizing OCT as a valuable tool for evaluating the creation of FLT outflow channels in the treatment of glaucoma.

Acknowledgements

Supported in part by grants from NIH/NEI R01 EY030304, NIH/NEI P30EY034070, an unrestricted grant from Research to Prevent Blindness, Inc. (RPB-203478), and a student research grant from American Society of Laser Medicine and Surgery (S0123).

References

1. Weinreb RN, Khaw PT. Primary open-angle glaucoma. Lancet. May 22 2004;363(9422):1711–20. doi:10.1016/S0140-6736(04)16257-0 [PubMed: 15158634]
2. Weinreb RN, Aung T, Medeiros FA. The pathophysiology and treatment of glaucoma: a review. JAMA. May 14 2014;311(18):1901–11. doi:10.1001/jama.2014.3192 [PubMed: 24825645]
3. Carreon T, van der Merwe E, Fellman RL, Johnstone M, Bhattacharya SK. Aqueous outflow - A continuum from trabecular meshwork to episcleral veins. Prog Retin Eye Res. Mar 2017;57:108–133. doi:10.1016/j.preteyeres.2016.12.004 [PubMed: 28028002]
4. Alm A, Nilsson SF. Uveoscleral outflow--a review. Exp Eye Res. Apr 2009;88(4):760–8. doi:10.1016/j.exer.2008.12.012 [PubMed: 19150349]
5. Johnson M, McLaren JW, Overby DR. Unconventional aqueous humor outflow: A review. Exp Eye Res. May 2017;158:94–111. doi:10.1016/j.exer.2016.01.017 [PubMed: 26850315]
6. Brubaker RF. Flow of aqueous humor in humans [The Friedenwald Lecture]. Invest Ophthalmol Vis Sci. Dec 1991;32(13):3145–66. [PubMed: 1748546]
7. Minckler D, Mosaed S, Francis B, Loewen N, Weinreb RN. Clinical results of ab interno trabeculotomy using the Trabectome for open-angle glaucoma: the mayo clinic series in Rochester, Minnesota. Am J Ophthalmol. Jun 2014;157(6):1325–6. doi:10.1016/j.ajo.2014.02.030 [PubMed: 24881841]
8. Samet S, Ong JA, Ahmed IIK. Hydrus microstent implantation for surgical management of glaucoma: a review of design, efficacy and safety. Eye Vis (Lond). 2019;6:32. doi:10.1186/s40662-019-0157-y [PubMed: 31660323]
9. Samuelson TW, Katz LJ, Wells JM, Duh YJ, Giamporcaro JE, Group USiS. Randomized evaluation of the trabecular micro-bypass stent with phacoemulsification in patients with glaucoma and cataract. Ophthalmology. Mar 2011;118(3):459–67. doi:10.1016/j.ophtha.2010.07.007 [PubMed: 20828829]
10. Durr GM, Toteberg-Harms M, Lewis R, Fea A, Marolo P, Ahmed IIK. Current review of Excimer laser Trabeculostomy. Eye Vis (Lond). 2020;7:24. doi:10.1186/s40662-020-00190-7 [PubMed: 32391398]
11. Greenwood MD, Seibold LK, Radcliffe NM, et al. Goniotomy with a single-use dual blade: Short-term results. J Cataract Refract Surg. Sep 2017;43(9):1197–1201. doi:10.1016/j.jcrs.2017.06.046 [PubMed: 28991617]
12. Mikula ER, Raksi F, Ahmed II, et al. Femtosecond Laser Trabeculotomy in Perfused Human Cadaver Anterior Segments: A Novel, Noninvasive Approach to Glaucoma Treatment. Transl Vis Sci Technol. Mar 2 2022;11(3):28. doi:10.1167/tvst.11.3.28
13. Mikula E, Holland G, Bradford S, et al. Intraocular Pressure Reduction by Femtosecond Laser Created Trabecular Channels in Perfused Human Anterior Segments. Transl Vis Sci Technol. Aug 2 2021;10(9):22. doi:10.1167/tvst.10.9.22
14. Nagy ZZ, Kranitz K, Ahmed IIK, De Francesco T, Mikula E, Juhasz T. First-in-Human Safety Study of Femtosecond Laser Image-Guided Trabeculotomy for Glaucoma Treatment: 24-month Outcomes. Ophthalmol Sci. Dec 2023;3(4):100313. doi:10.1016/j.xops.2023.100313
15. Juhasz T, Kastis GA, Suarez C, Bor Z, Bron WE. Time-resolved observations of shock waves and cavitation bubbles generated by femtosecond laser pulses in corneal tissue and water. Lasers Surg Med. 1996;19(1):23–31. doi:10.1002/(SICI)1096-9101(1996)19:1<23::AID-LSM4>3.0.CO;2-S [PubMed: 8836993]
16. Juhasz T, Kurtz R, Raksi F, Suarez C, Horvath C, Spooner G. The femtosecond blade: Applications in corneal surgery. Optics and Photonics News. 2002;13(1):24–29.
17. Juhasz T, Frieder H, Kurtz RM, Horvath C, Bille JF, Mourou G. Corneal refractive surgery with femtosecond lasers. Ieee J Sel Top Quant. Jul-Aug 1999;5(4):902–910. doi:Doi 10.1109/2944.796309
18. Ratkay-Traub I, Juhasz T, Horvath C, et al. Ultra-short pulse (femtosecond) laser surgery: initial use in LASIK flap creation. Ophthalmol Clin North Am. Jun 2001;14(2):347–55, viii-ix.

19. Palanker DV, Blumenkranz MS, Andersen D, et al. Femtosecond laser-assisted cataract surgery with integrated optical coherence tomography. Sci Transl Med. Nov 17 2010;2(58):58ra85. doi:10.1126/scitranslmed.3001305
20. Nagy ZZ, McAlinden C. Femtosecond laser cataract surgery. Eye Vis (Lond). 2015;2:11. doi:10.1186/s40662-015-0021-7 [PubMed: 26605364]
21. Luo S, Mikula ER, Bradford S, et al. Evaluating the Effect of Pulse Energy on Femtosecond Laser Trabeculotomy (FLT) Drainage Channels in Human Cadaver Eyes. Invest Ophthalmol Vis Sci. 2023;64(8):4896.
22. Mikula ER, Djotyan G, Luo S, Jester JV, Juhasz T. Femtosecond Laser Image Guided High-precision Trabeculotomy (FLigHT): a thermal collateral damage study. Invest Ophthalmol Vis Sci. 2023;64(8):4907.
23. He Y, Qu Y, Zhu J, et al. Confocal Shear Wave Acoustic Radiation Force Optical Coherence Elastography for Imaging and Quantification of the In Vivo Posterior Eye. IEEE J Sel Top Quantum Electron. Jan-Feb 2019;25(1)doi:10.1109/jstqe.2018.2834435
24. Toyran S, Liu Y, Singha S, et al. Femtosecond laser photodisruption of human trabecular meshwork: an in vitro study. Exp Eye Res. Sep 2005;81(3):298–305. doi:10.1016/j.exer.2005.02.001 [PubMed: 16129097]
25. Liu Y, Nakamura H, Witt TE, Edward DP, Gordon RJ. Femtosecond laser photodisruption of porcine anterior chamber angle: an ex vivo study. Ophthalmic Surg Lasers Imaging. Nov-Dec 2008;39(6):485–90. doi:10.3928/15428877-20081101-07 [PubMed: 19065979]
26. Tamm ER. The trabecular meshwork outflow pathways: structural and functional aspects. Exp Eye Res. Apr 2009;88(4):648–55. doi:10.1016/j.exer.2009.02.007 [PubMed: 19239914]
27. Nakamura H, Liu Y, Witt TE, Gordon RJ, Edward DP. Femtosecond laser photodisruption of primate trabecular meshwork: an ex vivo study. Invest Ophthalmol Vis Sci. Mar 2009;50(3):1198–204. doi:10.1167/iovs.07-1536 [PubMed: 18836174]
28. Luo S, Holland G, Khazaeinezhad R, Bradford S, Joshi R, Juhasz T. Iridocorneal angle imaging of a human donor eye by spectral-domain optical coherence tomography. Sci Rep. Aug 24 2023;13(1):13861. doi:10.1038/s41598-023-37248-0 [PubMed: 37620338]
29. Luo S, Holland G, Mikula E, et al. Dispersion compensation for spectral domain optical coherence tomography by time-frequency analysis and iterative optimization. Opt Contin. May 15 2022;1(5):1117–1136. doi:10.1364/OPTCON.455242
30. Mikula ER, Raksi F, Ahmed II, et al. Femtosecond Laser Trabeculotomy in Perfused Human Cadaver Anterior Segments: A Novel, Noninvasive Approach to Glaucoma Treatment. Translational Vision Science & Technology. 2022;11(3):28–28. doi:10.1167/tvst.11.3.28
31. Mikula E, Holland G, Srass H, Suarez C, Jester JV, Juhasz T. Intraocular Pressure Reduction by Femtosecond Laser Created Trabecular Channels in Perfused Human Anterior Segments. Transl Vis Sci Technol. Aug 2 2021;10(9):22. doi:10.1167/tvst.10.9.22

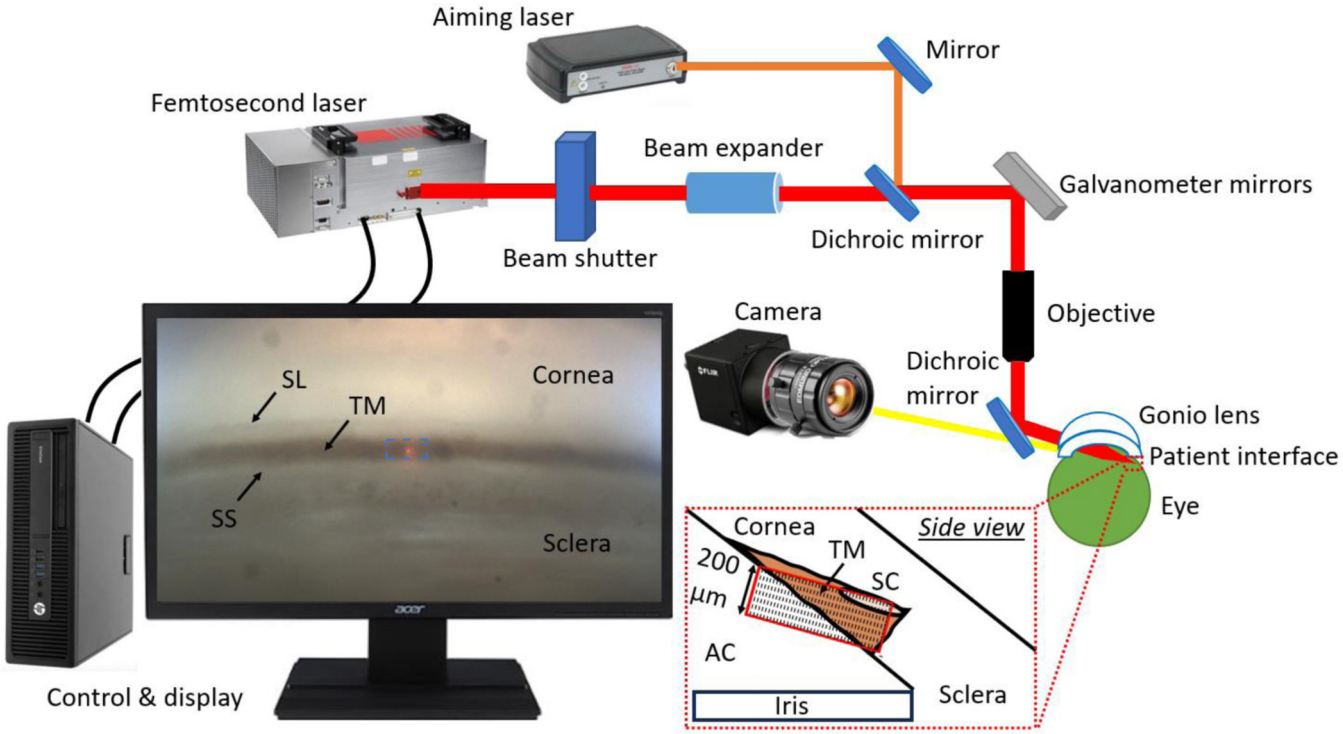

Fig. 1.

Components of the FLT surgical system. A commercial femtosecond laser is guided by a dual aiming beam, with the convergence of the dual beams indicating the focal point of the femtosecond laser on the trabecular meshwork (TM). The gonio camera light passes through a dichroic mirror, transmitting through a custom-built gonio lens, a custom-built patient interface, and the transparent cornea, ultimately focusing on the TM at the iridocorneal angle of a human eye. A typical goniolens view of the enucleated eye was shown on the control and display module's monitor. In the close-up schematic, the FLT laser scans across the entire TM, starting from inside SC and extending into the AC. The scan pattern is designed with a width of 500 μm and a height of 200 μm (blue dotted box in the gonioscopic image). Note that the 500 μm cutting width along the circumferential direction of the corneoscleral rim (perpendicular to the paper) is not depicted in the side view. FLT: femtosecond laser trabeculotomy; SL: Schwalbe's line; TM: trabecular meshwork; SC: Schlemm's canal; AC: anterior chamber.

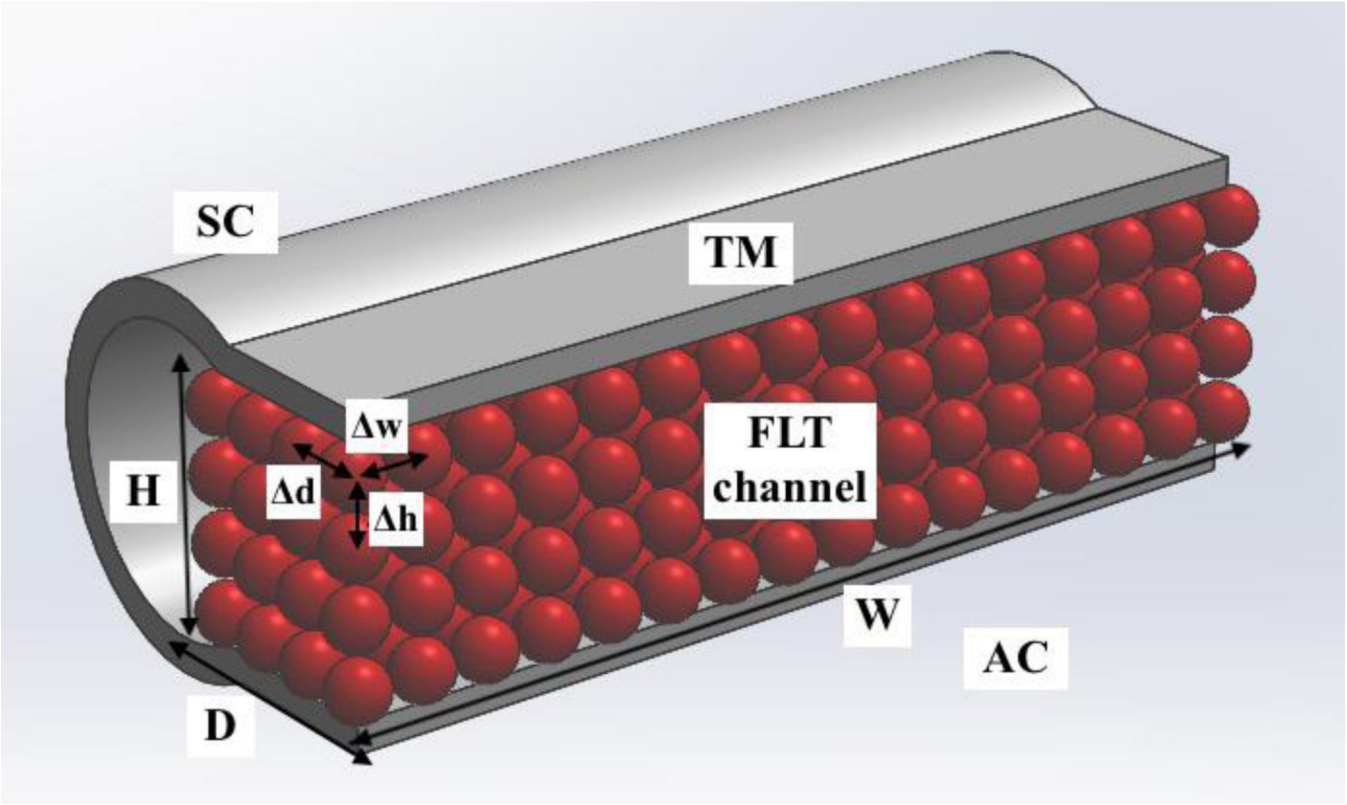

Fig. 2.

A schematic illustrating a femtosecond-created channel penetrating through the trabecular meshwork (TM), establishing a connection between the anterior chamber (AC) and Schlemm's canal (SC). The channel's geometry is determined by its width (W), height (H), and depth (D), while the laser spot, line, and layer separations are represented by Δw, Δh, and Δd, respectively. The red spots indicate the focal points of the femtosecond laser arranged in a raster pattern, effectively photodisrupting the TM tissues.

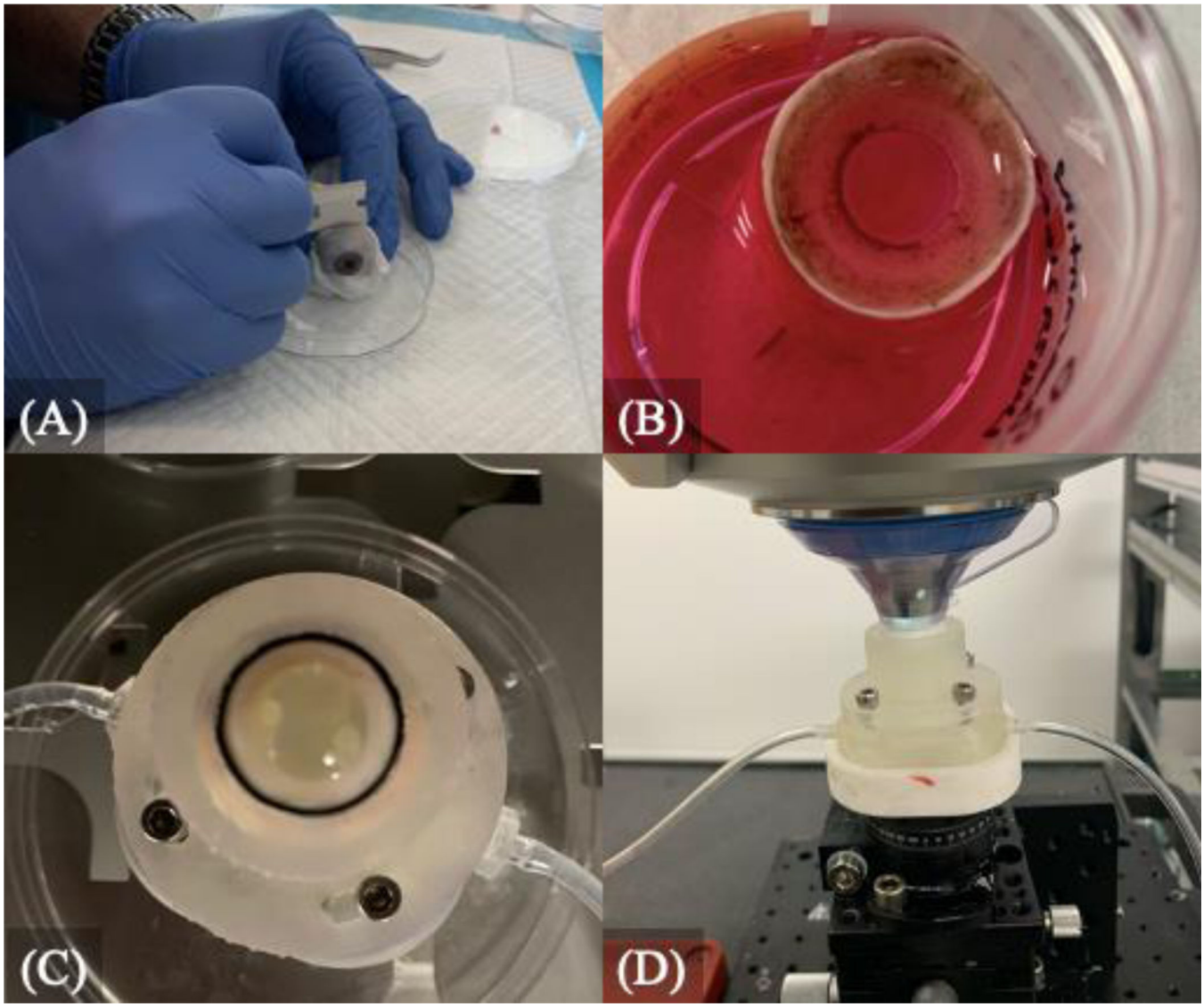

Fig. 3.

Sample preparation for FLT surgery. (A) Human donor eyes were obtained from the San Diego Eye Bank within 24 hours postmortem. (B) An anterior segment with an intact trabecular meshwork (TM) was dissected and (C) carefully mounted on a custom ocular perfusion device within an incubator. (D) The eye was docked to the FLT surgical system via a custom-built patient interface between the two. FLT: femtosecond laser trabeculotomy.

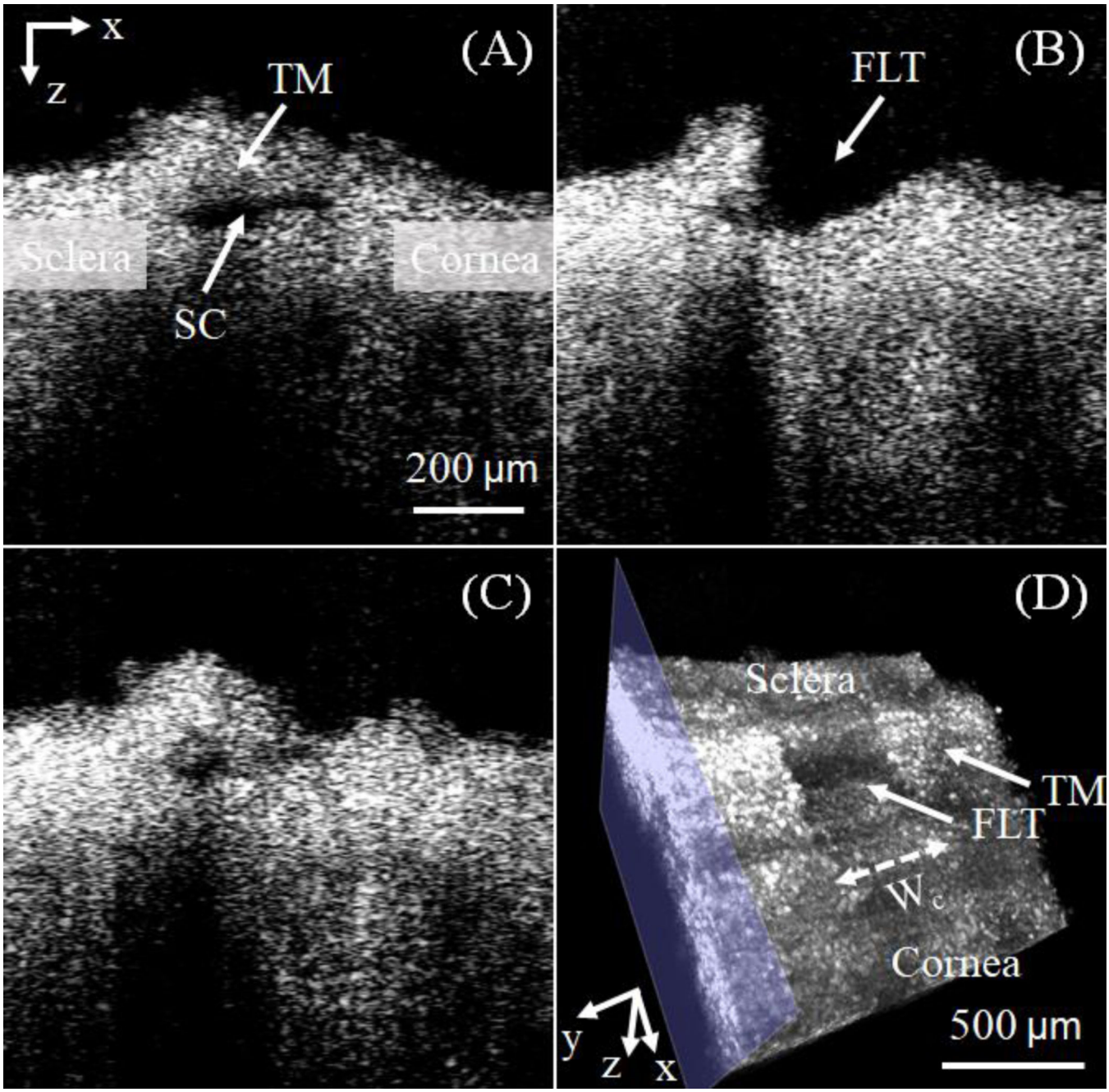

Fig. 4.

Representative OCT B-scan images at different slow-scanning locations and the 3D reconstructed image stack. As the sliding plane moves along the y-direction, the B-scan images show: (A) intact TM tissue, (B) a full-thickness cut creating an FLT channel connecting to Schlemm's canal, and (C) a partial-thickness cut in the TM tissue. The cutting width (W_c), analyzed from individual B-scans along the y-axis, serves as an evaluation metric detailed in Fig. 5. TM: trabecular meshwork; FLT: femtosecond laser trabeculotomy.

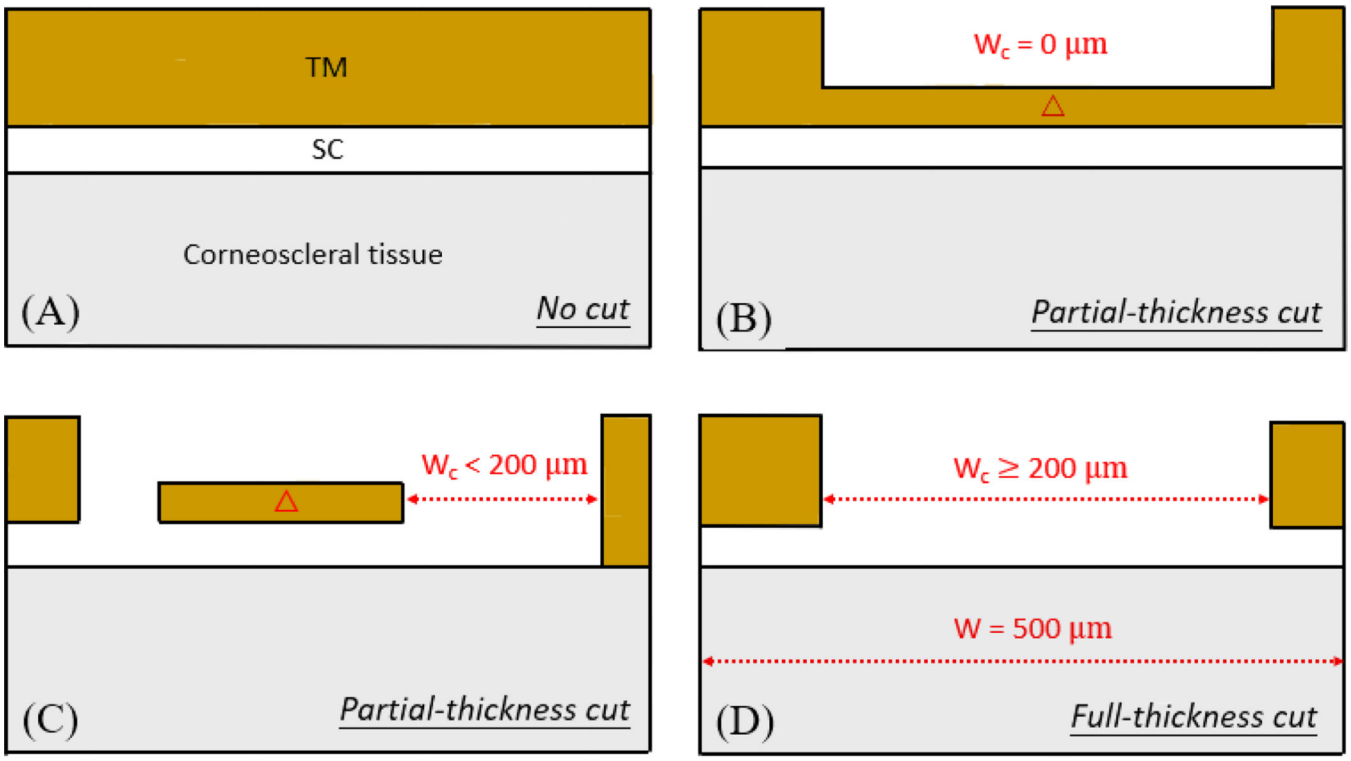

Fig. 5.

Illustration of FLT outflow channel evaluation. The 0 µm cutting width was considered when the TM is completely intact (A) or partially cut at any location along the circumferential direction (Y-axis) (B). A partial-thickness cut can also be defined as a maximum continuous cutting width (W_c) below 200 µm (C), while a full-thickness cut had a continuous cutting width of at least 200 µm (D). Marks '△' in (B) and (C) indicate an incomplete cut through the TM, preventing connections to SC, and were excluded from the cutting width calculation. FLT: femtosecond laser trabeculotomy; TM: trabecular meshwork; SC: Schlemm's canal.

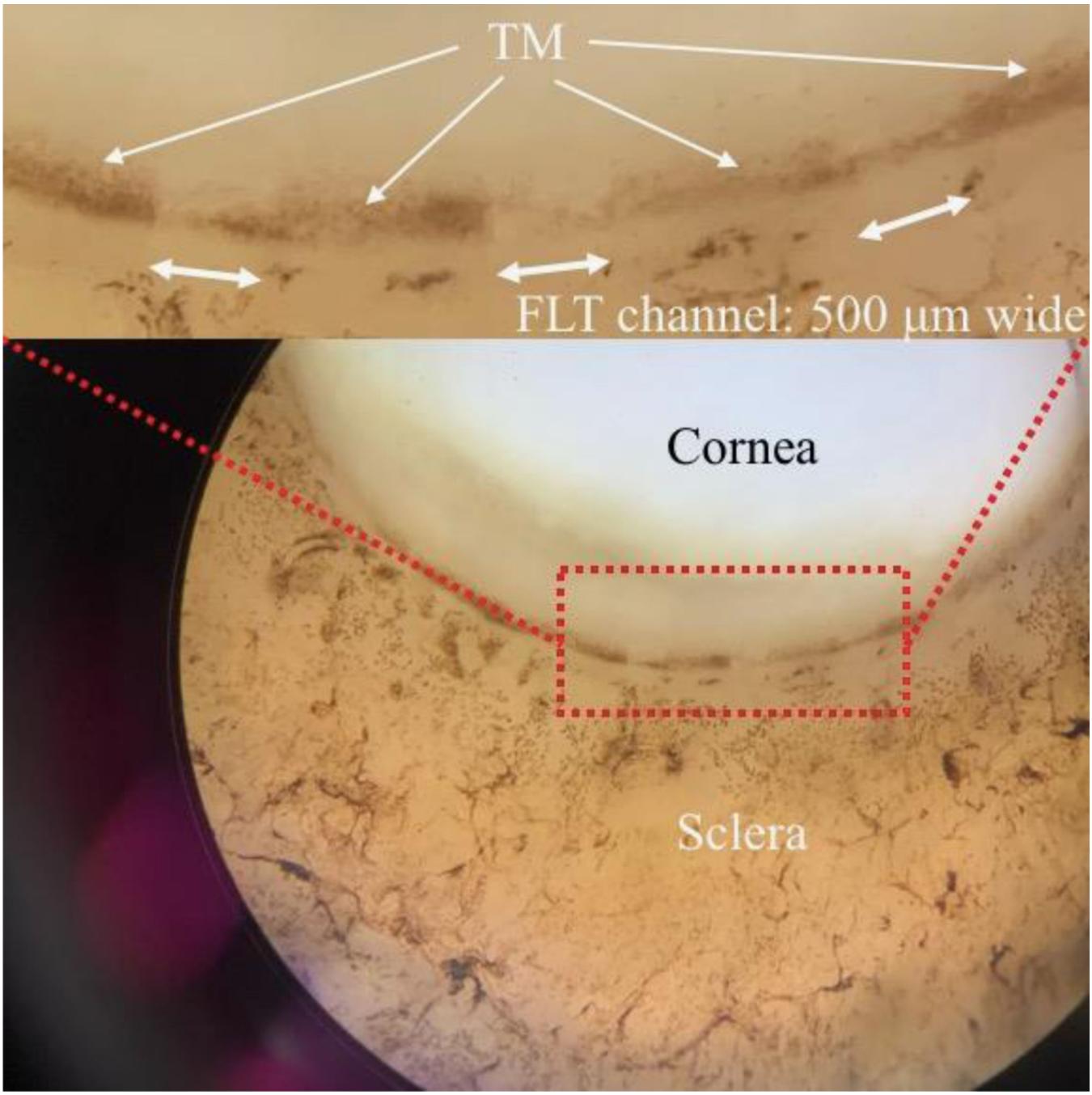

Fig. 6.

Three representative 500×200 μm^2 outflow channels (indicated by double arrows) created with 15 μJ energy through the brownish trabecular meshwork (TM), as observed under an optical microscope. FLT: femtosecond laser trabeculotomy.

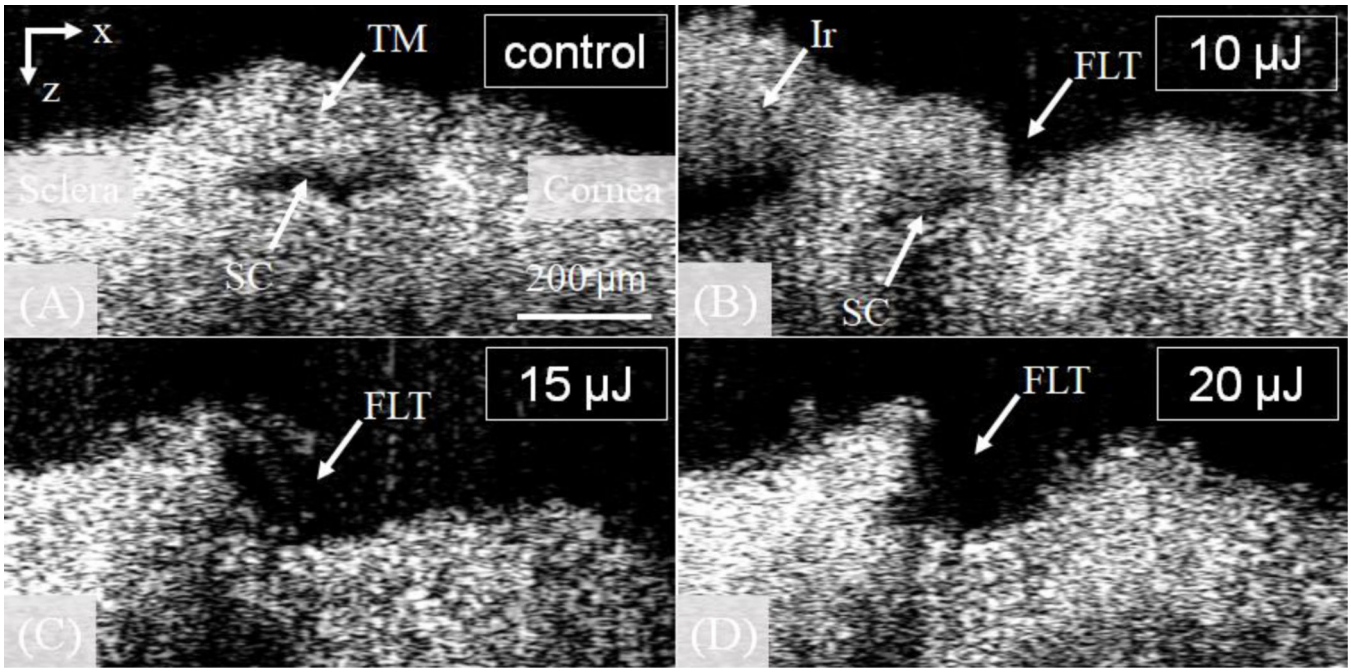

Fig. 7.

Sample OCT images of FLT outflow channels at varying pulse energies. At 10 μJ energy, a partial-thickness outflow channel is observed, while both 15 μJ and 20 μJ energies result in full-thickness channels. FLT: femtosecond laser trabeculotomy; TM: trabecular meshwork; SC: Schlemm's canal.

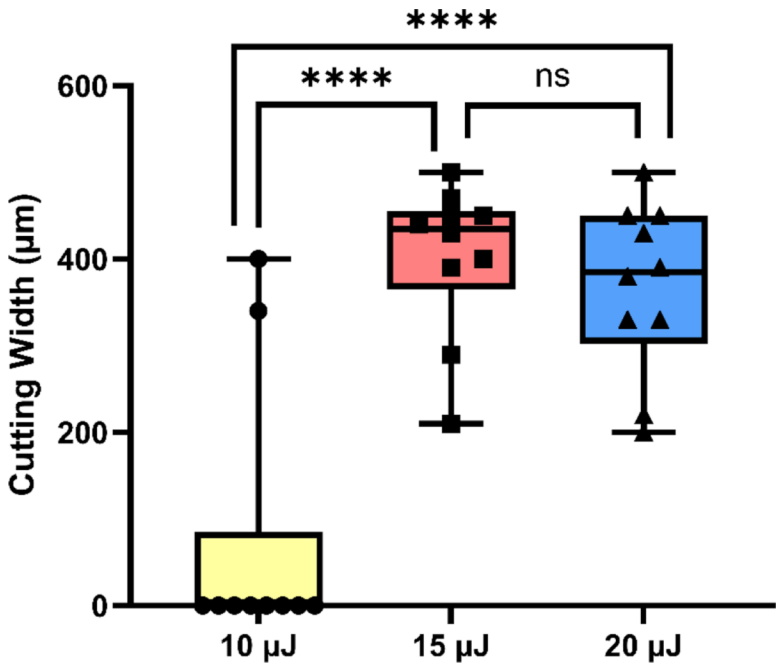

Fig. 8.

Statistics of the cutting width in the trabecular meshwork (TM) at different pulse energies. A significant difference in cutting width was observed both between 10 μJ and 15 μJ and between 10 μJ and 20 μJ (**** $P<0.0001$). However, there was no significant difference in the cutting width of the TM between 15 μJ and 20 μJ (ns, not significant: $P>0.05$). A pulse energy of 15 μJ is determined to be optimal for femtosecond laser trabeculotomy (FLT).

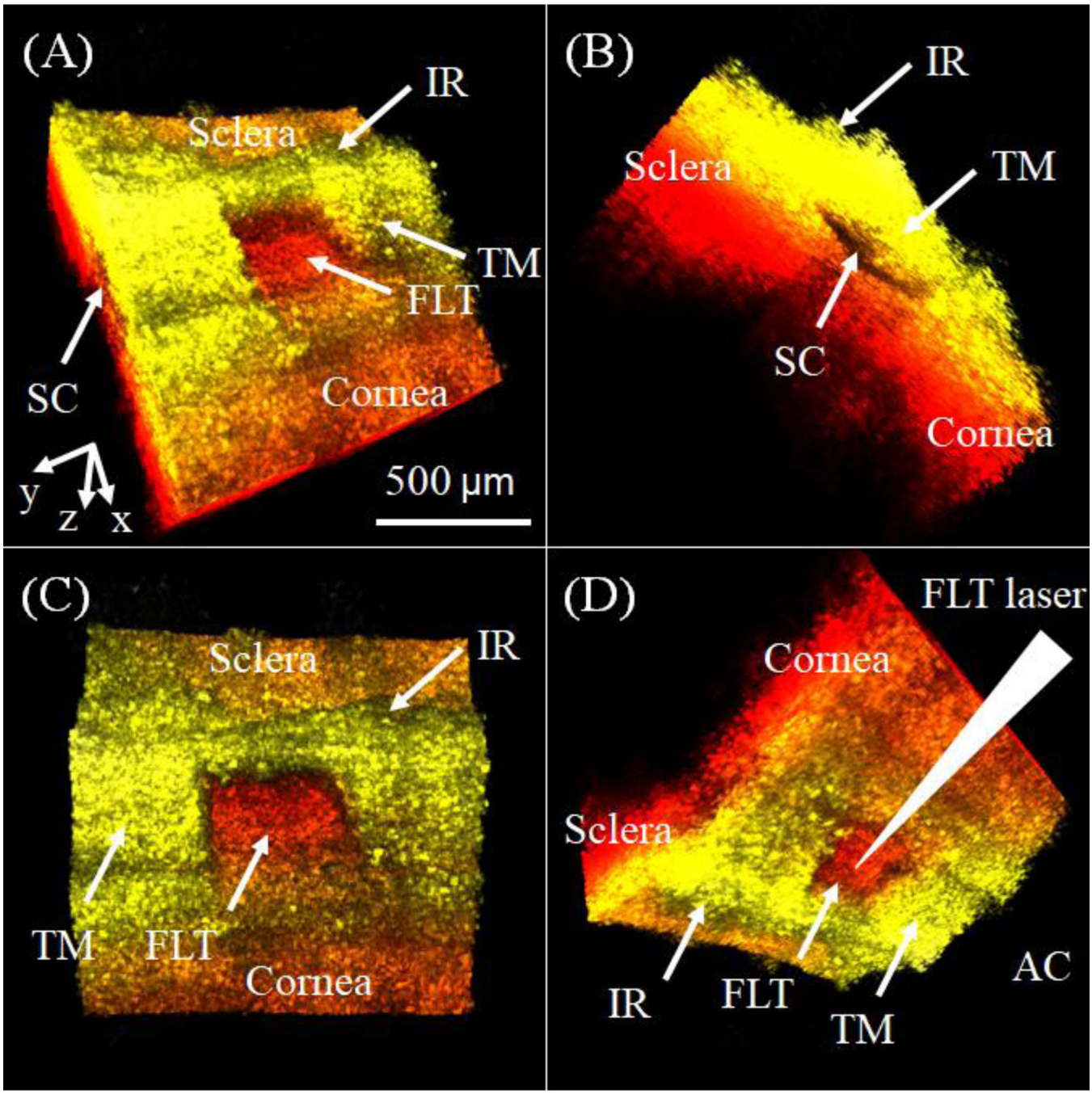

Fig. 9.

A representative 3D image stack of the iridocorneal angle, oriented from different perspectives, illustrates a wedge-shaped FLT outflow channel cut through the trabecular meshwork (TM) and extending into Schlemm's canal (SC). This channel was created using a pulse energy of 20 μJ, effectively establishing a direct connection between SC and the aqueous fluid in the anterior chamber (AC). The FLT channel and nearby structures were observed from (A) an approximately 45-degree view, (B) a side view, and (C) a top view.

The relationship between the angle structures and the FLT surgical laser is depicted in (D). FLT: femtosecond laser trabeculotomy; IR: iris root.

Table 1:

OCT Evaluation of FLT Channels Created at Different Pulse Energies

	10 μJ		15 μJ		20 μJ	
	Cutting width (μm)	**Result**	**Cutting width (μm)**	**Result**	**Cutting width (μm)**	**Result**
CH #01	0	No	390	Full	450	Full
CH #02	0	No	440	Full	330	Full
CH #03	0	No	470	Full	380	Full
CH #04	0	Partial	450	Full	200	Full
CH #05	340	Full	400	Full	330	Full
CH #06	400	Full	430	Full	450	Full
CH #07	0	No	500	Full	390	Full
CH #08	0	No	450	Full	430	Full
CH #09	0	Partial	290	Full	500	Full
CH #10	0	No	210	Full	220	Full